A simple co-precipitation/calcination method using PEG-1000 as solvent to formation of MWO_4 (M= Ba, Ca, Cd, Co, Cu, Mn, Ni, Pb, Sr, Zn) nanocrystals and their photocatalytic properties for degradation of industrial dyes

Ali Gholami, Ali Fosooni, Hadi Ghasemi

Department of Analytical Chemistry, Faculty of Chemistry, University of Kashan, Kashan, I. R. Iran

agholami@kashanu.ac.ir

Abstract

In this work, metal tungstate nano- and microcrystals (MWO_4) have been synthesized easily using simple co-precipitation route. PEG-1000 was used as good and cheap chelating agent to control the size and morphology of products. The synthesized metal tungstate crystals were characterized by available technique such as Fourier transform infrared (FT-IR) spectrum, X-ray diffraction (XRD) and scanning electron microscopy (SEM). To survey the photo catalyst properties of synthesized MWO_4, the photocatalytic degradation of some common dyes (Eriochrome Black T (EBT), Methylene Orange (MO), Methylene Blue (MB) which are present in industrial wastewaters was followed under UV-Vis light irradiation. The results showed that among prepared metal tungstate compounds, $PbWO_4$ has a higher total photocatalytic activity for degradation of mixed dyes (MB=91%, MO=94%, EBT=84%).

Keywords: Metal tungstate; Dye; Photocatalytic activity

Introduction

The number of new protocols and methods for synthesis of nanostructures are increasing day by day [1-2]. In the meantime, especially in recent years' tungstate nanocrystals have been considered in this area [3]. Literature review showed that these compounds have attracted huge concern in various fields such as electronics and electrical industries, healthcare, chemistry, biochemistry, engineering, and cosmetics [4-8]. Divalent transition metal tungstate's ($M^{II}WO_4$) have a wide application in fluorescent lamps, and lasers [9]. In addition to the mentioned items, some divalent species are considered due to their magnetic The number of new protocols and methods for synthesis of nanostructures are increasing day by day [1-2]. In the meantime, especially in recent years' tungstate nanocrystals have been considered in this area [3]. Literature review showed that these compounds have attracted huge concern in various fields such as electronics and electrical industries, healthcare, chemistry, biochemistry, engineering, and cosmetics [4-8]. Divalent transition metal tungstate's ($M^{II}WO_4$) have a wide application in fluorescent lamps, and lasers [9]. In addition to the mentioned items, some divalent species are considered due to their magnetic properties [10, 11] and electrical conductivity [12]. Also, this type of metal tungstate is used as catalyst and moisture sensor [13, 14].

The substitution of ions (M) with different size changes the crystal structure of MWO_4 due to the difference in unit cell dimensions. There are two types of MWO_4 structures, Wolframite-type monoclinic and Scheelite-type tetragonal structure. In Wolframite-type monoclinic structure, M^{2+} has ionic radii <0.77 Å (M^{2+}: Mn, Fe, Co, Ni, Zn, Mg), and tungsten atoms adopt hexagonal coordination. However, in Scheelite-type monoclinic structure, M^{2+} has ionic radii >0.99 Å (M^{2+}: Ba, Ca, Pb, Sr), and tungsten atoms adopt tetrahedral coordination [15, 16].

There are various proposed procedures for the preparation of MWO_4 nanocrystals (NPs) such as sol–gel, solid-state reaction, hydrothermal, aerosol pyrolysis, sputtering, Czochralski technique, solvothermal-mediated micro emulsion method, chemical bath deposition, metathetic reaction and co-precipitation processes [17-34].

In recent decades, the contamination of environment has been specified as one of the major issues of modern society, mainly due to significant population and industry growth [35]. Among the various industries that generate large volumes of wastewater, the textile industries have a special place due to high consumption of water during the processes of dyeing [36].

There are conventional technologies currently used to degrade textile wastewater that are based on adsorption, reverse osmosis/membrane filtration, coagulation/flocculation and electrocoagulation [37]. However, the above methods are not high efficient because these techniques are non-destructive, and do not cause complete degradation. In this regard, advanced oxidation processes (AOPs) using heterogeneous photocatalysis can produce active species leading to the total degradation of most of organic pollutants. AOPs are based on creation of reactive species such as hydroxyl radicals ($OH^{\cdot}$) that oxidize and destruct a wide range of organic pollutants rapidly [38].

As mentioned earlier, there are different presented protocols for synthesis of tungstate nanostructures; however, there is still a need for more simple and affordable procedures. Besides, the wide range of transition metal oxide can be effective in photodegradation of dyes [39]. The various researches confirm that like other transition metals, metal tungstates are promising category as photocatalyst candidate [40]. Based on above discussions, the presentation of easy and cheap protocol for synthesis of tungstates compound family and their application for photodegradation of some dyes are interesting. In the present work, we report facile and simple protocol for synthesis of MWO_4 nano- and microcrystals using suitable and available chelating agent. In the next step, the ability of these structures in the degradation of common industrial wastewater dyes, especially textile wastewater dyes were investigated.

Results and Discussion

In wolframite structures MWO_4 (M = Fe, Mn, Ni, Cd, Zn, Cu, and Mg), W_2O_8 groups are major structural unit in their chemical structures [41]. However, the absorption peaks with the maxima at 890 cm^{-1} could be related to the vibration frequencies of tungsten-oxygen (W-O) bonds in tetrahedral WO_4 unit [42]. The FT-IR spectra of MWO_4 crystals is presented in Fig. 1.

The tungsten-oxygen (W-O) stretching vibration frequencies of MWO_4 crystals (M= Ba, Ca, Cd, Co, Cu, Mn, Ni, Pb, Sr, Zn) appeared at 783, 769, 822, 826, 821, 821, 825, 747, 783, 840 cm^{-1}, respectively. The vibrational frequency of chemical bond is directly proportional to the bond strength. As result the higher the bond strength, the higher the frequency of vibration. It can be easily understanding the effect of used metal on the bond strength by comparing the vibrational frequency number of the W-O bond (W-O Bond strength: Zn>Co> Ni>Cd> Cu ≈ Mn>Sr ≈ Ba>Ca>Pb).

In order to proof the chemical structure of the samples, X-ray diffraction (XRD) analysis was performed and results were shown in Fig. XRD patterns unveiled which all nanostructure is crystalline and pure. Based on XRD data, the diameter of as-prepared nanocrystals (MWO_4, M= Co, Zn, Ni, Mn, Cu, and Ca) are calculated to be less than 200 nm using the Scherer Eq. The other structures had large sizes and they can be considered as microstructure (MWO_4, M= Ba, Cd, Pb, and Sr). The particle diameters obtained from XRD are consistent with the SEM observations. In general, the metal tungstates M= Mn, Co, Zn, Ni and M= Ba, Sr, Ca, Pb crystallize with the wolframite and scheelite-type structure, respectively. However, $CuWO_4$ shows a different pattern from the other wolframite-type structures due to a distorted structure [5]. In copper tungstate Jahn-Teller distortion causes the elongation of CuO_6 octahedra units and the copper atoms substantially dislocated from the center of the octahedra [43].

In order to prevent the aggregation of crystals and control the size of structures, using chelating agent is useful [44, 45]. In this work, to achieve appropriate size particle, PEG-1000 as a chief and non-toxic chelating agent was used. The SEM images of metal tungstates (M= Ba, Ca, Cd, Co, Cu, Mn, Ni, Pb, Sr, Zn) are shown in Fig. 3. The SEM images presented in the Fig. 3 disclosed that the morphology of samples Mn, Ba, Ni, Cu, Ca, Zn, Co, Sr, Cd is particle-like, and Pb is porous spindle-like. Comparing the obtained results showed that except for microstructures, the remaining samples have nanometer dimensions. The final products mainly consist of crystals with average particle size under 200 nm. In total, the SEM images showed that PEG-1000 causes particle-like structure. To measure the

photocatalytic activity of the prepared MWO_4 structures, the photocatalytic degradation of mixed dyes (MB, MO, and EBT) as an example of waste from industrial plants was surveyed under UV-Visible light irradiation (λ= 250-800 nm).

The absorbance spectra of dye solution were recorded with an UV–Vis spectrophotometer. The de-colorization efficiency (%) was calculated according to following equation:

(DE %) = $\frac{C_0-C}{C_0}\times 100$, (DE=De-colorization efficiency)

The results for degradation process were very promising (Table 1). It is clear from table 1 that the least amount of degradation is for $BaWO_4$/EBT (60%) and the most amount of degradation is for $PbWO_4$/EBT (94%). Comparison of the decomposition efficiency for each structures revealed that lead tungstate had the best performance. The dye degradation process was proceeded without using visible light irradiation or nano- and microcrystalline MWO_4 and there was not observed considerable dye degradation process.

Based on previous reports as well as the chemical character of the prepared tungstate compounds, we concluded that the self-degradation of organic dye under visible light was not major route. Thus, the acceptable mechanism for photocatalytic degradation of mentioned dyes is presented in Scheme 1.

The heterogeneous photocatalytic process includes several expected sections such as adsorption, diffusion, and reaction. In this work, it is understood that the enhanced photocatalytic activity can be related to suitable distribution and size of the pore in the structure of surface tungstate, and high hydroxyl amount.

Table 1. The comparison of photocatalytic degradation of mixed dyes by MWO_4 nano- and microcrystals

MWO_4	Decolorization MB (%)	Decolorization MO (%)	Decolorization EBT (%)
$MnWO_4$	91	83	93
$BaWO_4$	84	75	60
$NiWO_4$	87	66	83
$CuWO_4$	91	76	92
$CaWO_4$	90	92	85
$ZnWO_4$	89	75	79
$CoWO_4$	78	73	89
$SrWO_4$	91	90	79
$PbWO_4$	91	94	84
$CdWO_4$	88	84	79

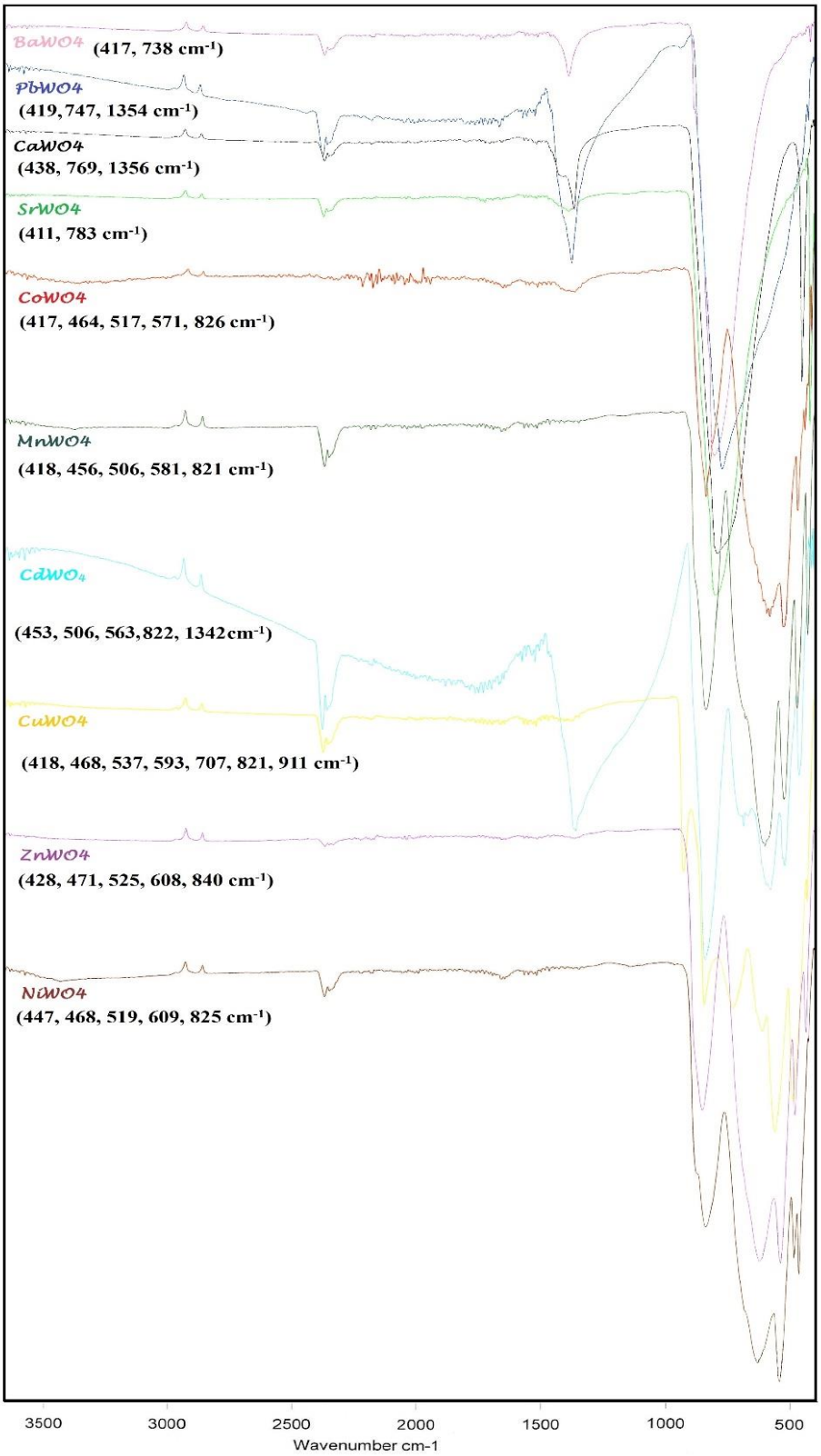

Fig. 1 FT-IR spectrum of MWO_4 crystals

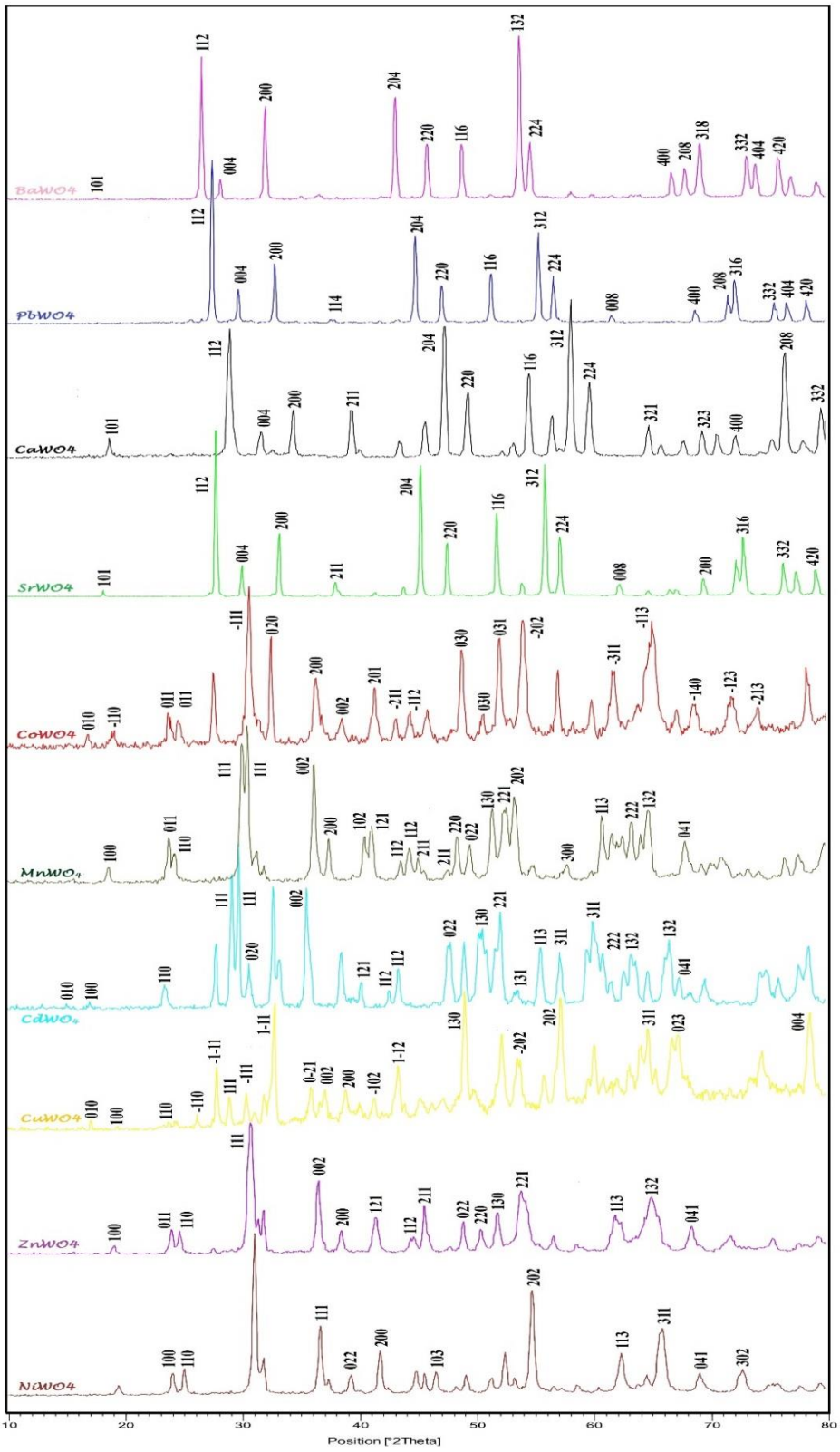

Fig. 2 XRD patterns of MWO_4 crystals

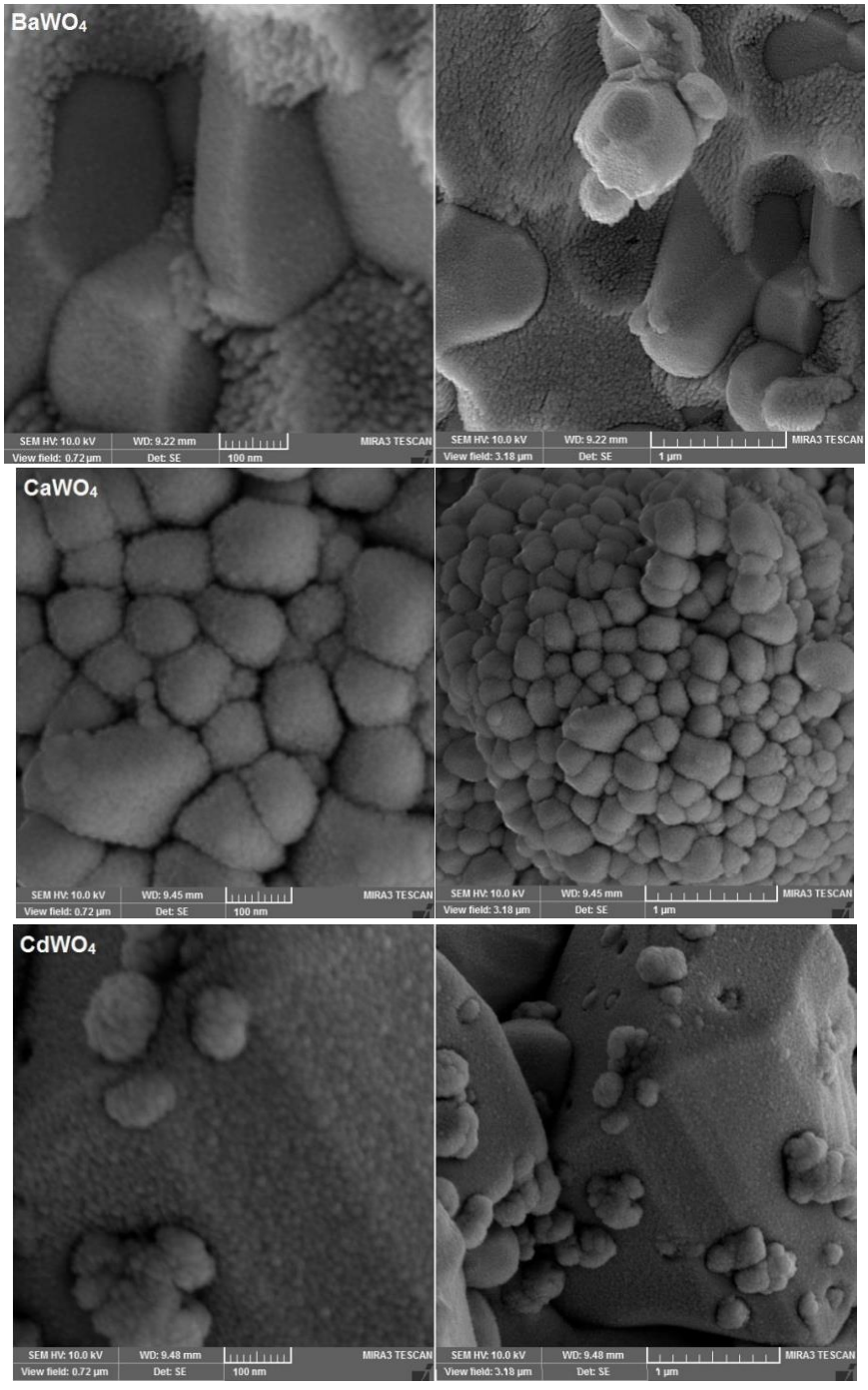
BaWO4
SEM HV: 10.0 kV
WD: 9.22 mm
MIRA3 TESCAN
View field: 0.72 µm
Det: SE
100 nm
SEM HV: 10.0 kV
WD: 9.22 mm
MIRA3 TESCAN
View field: 3.18 µm
Det: SE
1 µm
CaWO4
SEM HV: 10.0 kV
WD: 9.45 mm
MIRA3 TESCAN
View field: 0.72 µm
Det: SE
100 nm
SEM HV: 10.0 kV
WD: 9.45 mm
MIRA3 TESCAN
View field: 3.18 µm
Det: SE
1 µm
CdWO4
SEM HV: 10.0 kV
WD: 9.48 mm
MIRA3 TESCAN
View field: 0.72 µm
Det: SE
100 nm
SEM HV: 10.0 kV
WD: 9.48 mm
MIRA3 TESCAN
View field: 3.18 µm
Det: SE
1 µm

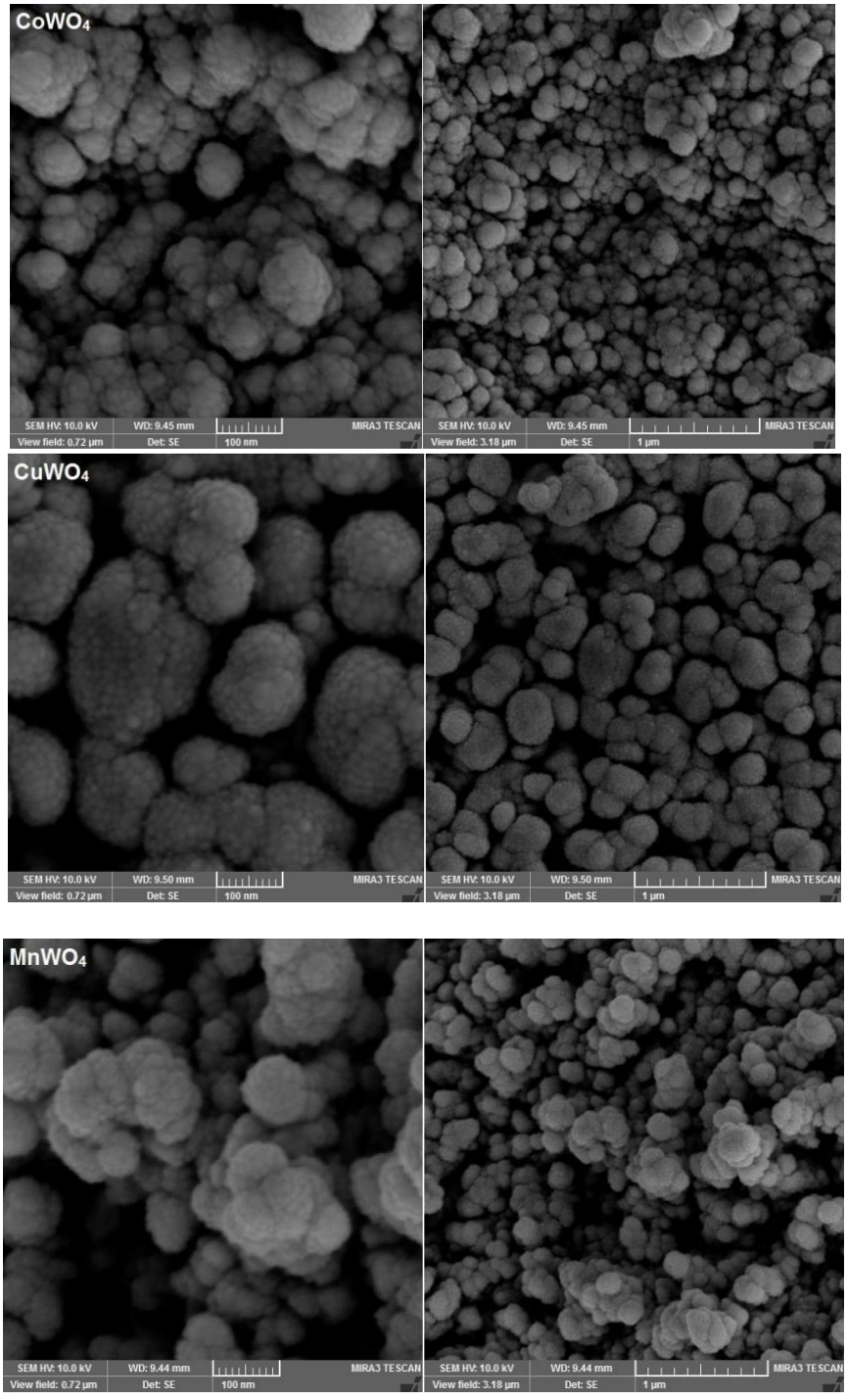
CoWO4
SEM HV: 10.0 kV
WD: 9.45 mm
MIRA3 TESCAN
View field: 0.72 µm
Det: SE
100 nm
SEM HV: 10.0 kV
WD: 9.45 mm
MIRA3 TESCAN
View field: 3.18 µm
Det: SE
1 µm
CuWO4
SEM HV: 10.0 kV
WD: 9.50 mm
MIRA3 TESCAN
View field: 0.72 µm
Det: SE
100 nm
SEM HV: 10.0 kV
WD: 9.50 mm
MIRA3 TESCAN
View field: 3.18 µm
Det: SE
1 µm
MnWO4
SEM HV: 10.0 kV
WD: 9.44 mm
MIRA3 TESCAN
View field: 0.72 µm
Det: SE
100 nm
SEM HV: 10.0 kV
WD: 9.44 mm
MIRA3 TESCAN
View field: 3.18 µm
Det: SE
1 µm

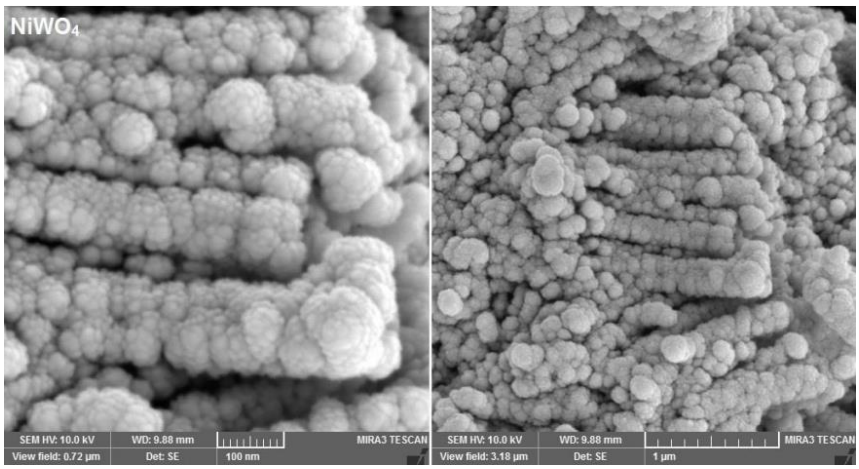
NiWO4
SEM HV: 10.0 kV
WD: 9.88 mm
MIRA3 TESCAN
View field: 0.72 µm
Det: SE
100 nm
SEM HV: 10.0 kV
WD: 9.88 mm
MIRA3 TESCAN
View field: 3.18 µm
Det: SE
1 µm

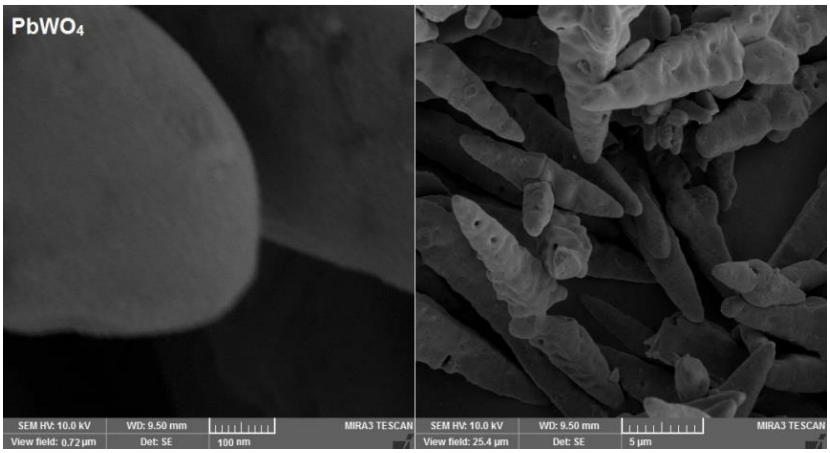
PbWO4
SEM HV: 10.0 kV
WD: 9.50 mm
MIRA3 TESCAN
View field: 0.72 µm
Det: SE
100 nm
SEM HV: 10.0 kV
WD: 9.50 mm
MIRA3 TESCAN
View field: 25.4 µm
Det: SE
5 µm

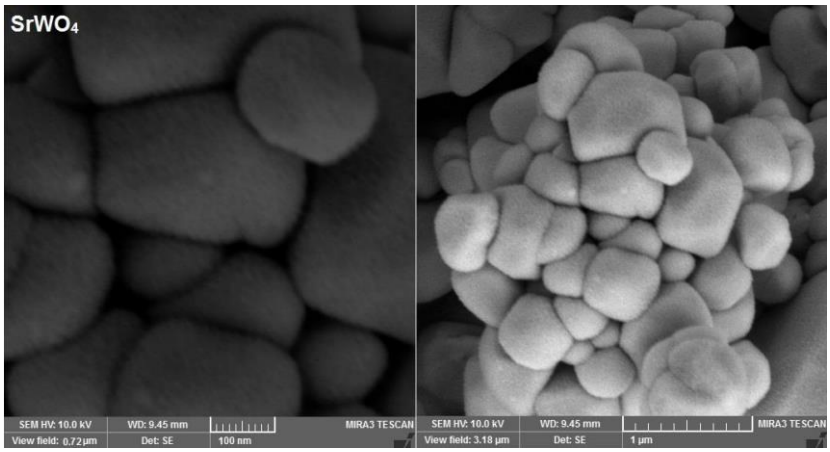
SrWO4
SEM HV: 10.0 kV
WD: 9.45 mm
MIRA3 TESCAN
View field: 0.72 µm
Det: SE
100 nm
SEM HV: 10.0 kV
WD: 9.45 mm
MIRA3 TESCAN
View field: 3.18 µm
Det: SE
1 µm

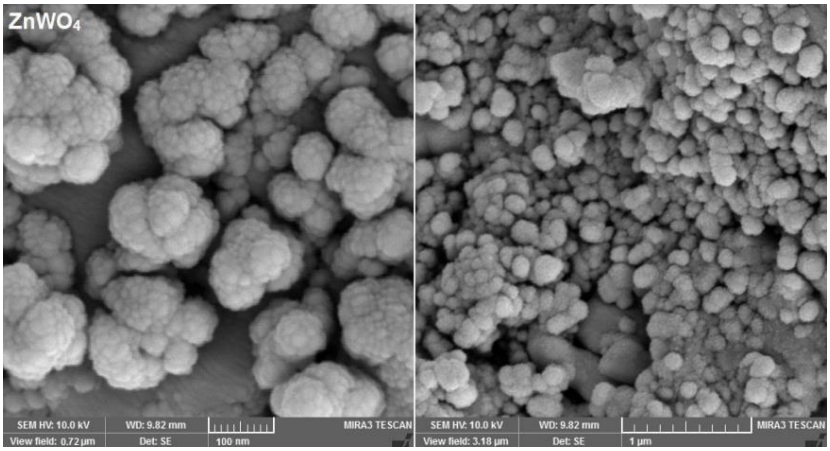

Fig. 3 SEM images of MWO_4 crystals

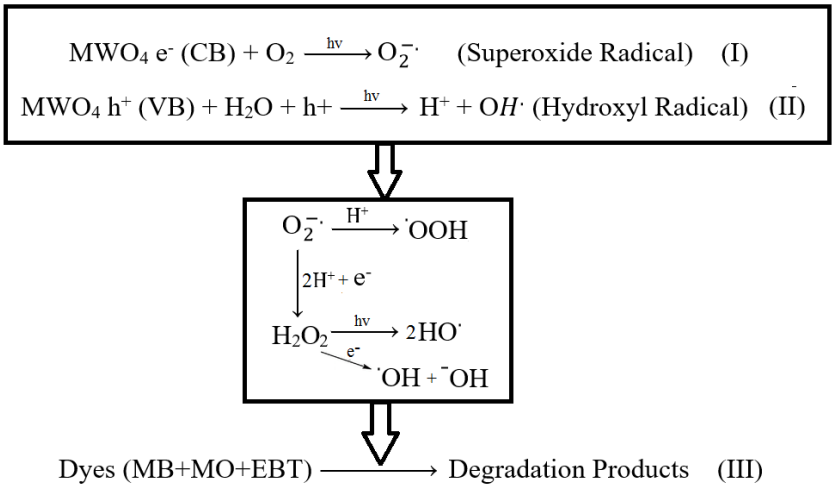

Scheme 1 Proposed reaction mechanism steps for degradation of dyes

Conclusion

In conclusion, wide range of MWO_4 Nano- and microcrystals have been easily and synthesized from $Na_2WO_4.2H_2O$ and $M(NO_3)_n.mH_2O$ by a simple co-precipitation method. In order to achieve the proper size of crystals, PEG-1000 as cheap chelating agent was used. MWO_4 Nano- and microcrystals were characterized by FT-IR, XRD, and SEM. In order to investigate the photocatalytic properties of synthesized structures, photo degradation of dyes was investigated. A mixture of three common dyes (Eriochrome Black T (EBT), Methylene Orange (MO), Methylene Blue (MB) as available dyes in industrial wastewater was exposed to UV-Visible light in the presence of synthesized photo catalysts. All of the prepared structures showed a good ability to destroy industrial dyes. The best results for mixed dyes degradation under irradiation of visible light were disclosed for $PbWO_4$ (MB=91%, MO=94%, EBT=84%). The results for lead acetate species that has micro dimensions confirm that here the chemical nature and ability to produce active species are important more than the particle size of photo catalyst.

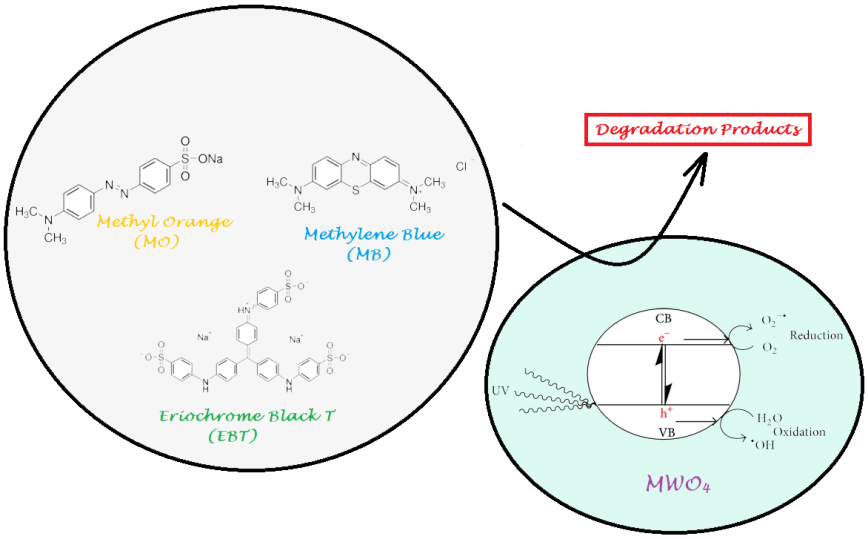

Fig. 4 The photo degradation reaction mechanism of dyes under visible light irradiation

Experimental

Characterization

$Na_2WO_4.2H_2O$, $M(NO_3)_n \bullet mH_2O$ (M=Mn, Ba, Ni, Cu, Ca, Zn, Co, Sr, Pb, Cd), and polyethylene glycol-1000 (PEG-1000) were purchased from Merck Company. All the chemicals used in this method were of analytical grade and used as-received without any further purification. X-ray diffraction (XRD) patterns were recorded by a Philips-X'PertPro, X-ray diffractometer using Ni-filtered Cu Ka radiation at scan range of 10 \ 2h\ 80. Scanning electron microscopy (SEM) images were obtained on LEO-1455VP equipped with an energy dispersive X-ray spectroscopy. Fourier transform infrared (FT-IR) spectrum was recorded on a magna Nicolet 550 spectrophotometer in KBr pellets. Spectroscopy analysis (UV–Vis) was carried out using Shimadzu spectrometer (Diffuse reflectance UV-vis spectroscopy). The energy dispersive spectrometry (EDS) analysis was studied by XL30, Philips microscope.

Synthesis of MWO_4 crystals

In a typical synthesis, the stoichiometric amount of $M(NO_3)_2 \cdot 6H_2O$ (1mmol) was dissolved in 30 ml distilled water under stirring to form a homogeneous solution. Afterwards, 1 m/mol of $Na_2WO_4.2H_2O$ and PEG as surfactant were dissolved in 60 ml distilled water and was added to the above solution under constant stirring. Finally, the white precipitate was filtered and washed three times with distilled water. The final product was dried at 60 $^{\circ}C$ and then calcined at 500 $^{\circ}C$ for 60 min in a conventional furnace in air atmosphere.

Photocatalytic experimental

To evaluate the photocatalytic activities of prepared MWO_4 Nano- and microcrystals, the photo degradation of mixed dyes solution including MB, MO, and EBT was examined as a model reaction under UV-Visible light irradiation. 0.025 g of the catalyst was suspended in 50 mL of mixed dye solution. In order to reach adsorption equilibrium, the mixture was aerated for 30 minutes. A xenon arc lamp (500W) was used as UV-Visible light irradiation source at room temperature. After 120 minutes, an adequate amount of the mixture was withdrawn and the photo catalyst was separated from the solution and was analyzed by a UV–Vis spectrometer.

Acknowledgements

Authors gratefully acknowledge the financial support from University of Kashan for providing support to undertake this work.

References

1. Gawande M. B., Goswami A., Asefa T., Guo H., Biradar A. V., Peng D-L., Zboril R. and Varma R. S., Chemical Society Reviews, 2015, 44, 7540.
2. Gawande Mano. B., Goswami A., Felpin F-X., Asefa T., Huang X., Silva R., Zou X., Zboril R., and Varma R. S., Chemical Reviews, 2016, 116(6), 3722.
3. Kaczmareka, A. M. and Deun R. V., Chemical Society Reviews, 2013, 42, 8835.
4. Jiang Y., Liu B., Zhai Z., Liu X., Yang B., Liu L., Jiang X., Applied Surface Science, 2015, 356, 273.
5. Ungelenka J., Speldrichb M., Dronskowskib R., Feldmann C., Solid State Sciences, 2014, 31, 62.
6 Feng W-L., Tao C-Y., Wang K., Spectroscopy Letters, 2015, 48, 381.
7. El-Sheikh S. M., Rashad M. M., Journal of Cluster Science, 2015, 26, 743.
8. Peng T., Liu C., Hou X., Zhang Z., Wang C., Yan H., Lu Y., Liu X., Luo Yo., Electrochimica Acta, 2017, 224, 460.
9. Zawawi S. M. M., Yahya R., Hassan A., Mahmud H. N. M. E., Daud M. N., Chemistry Central Journal, 2013, 7, 80.
10. Van Uitert L. G., Sherwood R. C., Williams H. J., Rubin J. J., Bonner W. A., Journal of Physics and Chemistry of Solids, 1964, 25, 1447.
11. Lake B., Cowley R. A., Tennant D.A., Journal of Physics: Condensed Matter, 1997, 49, 10951.
12. Mathew T., Batra N.M., Arora S.K., Journal of Materials Science, 1992, 27, 4003.
13. Tamaki J., Fujii T., Fujimori K., Miura N., Yamazoe N., Sensors and Actuators B: Chemical, 1995, 24, 396.
14. Stern D. L., Grasselli R. K., Journal of Catalysis, 1997, 167, 570.
15. Yu S. H., Liu B., Mo M. S., Huang J. H., Li X. M., Qian Y. T., Advanced Functional Materials, 2002, 13, 639.
16. Hongbo F., Shaogui Y., Shicheng Z., Zhijian Z., Journal of Applied Spectroscopy, 2009, 76, 227.
17. Nishigaki S., Yano S., Kato H., Nonomura T., Journal of the American Ceramic Society, 1988, 71, C-11 ().
18. Cavalcante L. S., Batista F. M. C., Almeida M. A. P., Rabelo A. C., Nogueira I. C., Batista N. C., Varela J. A., Santos M. R. M. C., Longobd E. and Li M. Siu, RSC Advances., 2012, 2, 6438.
19. Cavalcante L. S., Sczancoski J. C., Batista N. C., Longoa E., Varela J. A., Orlandi M. O., Advanced Powder Technology, 2013, 24, 344.
20. Chena H. and Xu Y., RSC Advances, 2015, 5, 8108.
21. Liang L., Liu H., Tiana Y., Haoa Q., Liua C., Wangb W., Xie X., Materials Letters, 2016, 182, 302.
22. Guo Y., Zhang G., Gana H. and Zhang Y., Dalton Transactions, 2012, 41, 12697.
23. Huang G., Zhang C., Zhu Y., Journal of Alloys and Compounds, 2007, 432, 269.
24. Vosoughifar M., Journal of Materials Science: Materials in Electronics, 2017, 28, 2135.
25. Hao Y., Zhang L., Zhang Y., Zhaoa L. and Zhang B., RSC Advances, 2017, 7, 26179.
26. AlShehri S. M., Ahmed J., Alzahrania A. M. and Ahamada T., New Journal of Chemistry, 2017, 41, 8178.
27. AlShehri S. M., Ahmed J., Basheer T. A., Almaswari M., Khan A., Journal of Nanoparticle Research, 2017, 19, 289.
28. Cho W. S., Yoshimura M., Japanese Journal of Applied Physics, 1997, 36, 1216.
29. Esaka T., Solid State Ionics, 2000, 136–137, 1.
30. Zhai R., Wang H., Yan H., Yoshimura M., Journal of Crystal Growth, 2006, 647, 289.
31. Basiev T. T., Sobol A. A., Voronko Y. K., Zverev P. G., Optical Materials, 2000, 15, 205.
32. Sun L., Guo Q., Wu X., Luo S., Pan W., Huang K., Lu J., Ren L., Cao M., Hu C., Journal of Physical Chemistry C, 2007, 111, 532.
33. Thangadurai V., Knittlmayer C., Weppner W., Materials Science and Engineering: B, 2004, 106, 228.
34. Sen A., Pramanik P., Journal of the European Ceramic Society, 2001, 21, 745.
35. Colpini L. M. S., Lenzi G. G., Urio M. B., Kochepka D. M., Alves H. J., Journal of Environmental Chemical Engineering, 2014, 2, 2365.
36. Hernández-Rodríguez M. J., Fernández-Rodríguez C., Donã-Rodríguez J. M., González-Díaz O. M., Zerbani D., Pérez Penã J., Journal of Environmental Chemical Engineering, 2014, 2, 163.

37. Souza R. P., Domingues F. S., Pezoti O., Ambrosio E., Ferrari-Lima A. M., Garcia J. C., Journal of Photochemistry and Photobiology A: Chemistry, 2016, 329, 9.
38. Daneshvar N., Salari D., Khataee A.R., Journal of Photochemistry and Photobiology A: Chemistry, 2004, 162, 317.
39. Chen C., Maa W., Zhao J., Chemical Society Reviews, 2010, 39, 4206.
40. López X. A., Fuentes A. F., Zaragoza M. M., Guillén J. A. D., Gutiérrez J. S., LópezOrtiz A., Collins-Martínez V., International Journal of Hydrogen Energy, 2016, 41, 23312.
41. Khyzhun O. Y., Bekenev V. L., Solonin Y. M., Journal of Alloys and Compounds, 2009, 184, 480.

42. Pourmortazavi S. M., Rahimi-Nasrabadi M., Khalilian-Shalamzari M., Ghaeni H. R., Hajimirsadeghi S. S., Journal of Inorganic and Organometallic Polymers and Materials, 2014, 24, 333.
43. Kihlborg L., Gebert E., Acta Crystallographic, 1970, 26, 1020.
44. Müllera J., Bauera K. N., Prozellera D., Simona J., Mailändera V., Wurma F. R., Winzena S., Landfester K., Biomaterials, 2017, 115, 1.
45. Ebrahiminezhad ,, Taghizadeh S, , Berenjian A, , Heidaryan Naeini F., Ghasemi Y, , Journal of Nanoscience and Nanotechnology, 2017, 7, 104.